

LA-6615

295
19-29-77

1448
UC-20 and UC-34a

Issued: September 1977

Photoionization Cross Sections and Radiative Recombination Rate Coefficients for Positive Ions of Carbon and Gold

W. D. Barfield



UNITED STATES
ENERGY RESEARCH AND DEVELOPMENT ADMINISTRATION
CONTRACT W-7405-ENG. 36

DISTRIBUTION OF THIS DOCUMENT IS UNLIMITED

PHOTOIONIZATION CROSS SECTIONS AND RADIATIVE
RECOMBINATION RATE COEFFICIENTS FOR POSITIVE IONS OF CARBON AND GOLD

by
W. D. Barfield

NOTICE
This report was prepared as an account of work sponsored by the United States Government. Neither the United States nor the United States Energy Research and Development Administration, nor any of their employees, nor any of their contractors, subcontractors, or their employees, makes any warranty, express or implied, or assumes any legal liability or responsibility for the accuracy, completeness or usefulness of any information, apparatus, product or process disclosed, or represents that its use would not infringe privately owned rights.

ABSTRACT

Partial photoionization cross sections based on a nonhydrogenic single-electron model that utilizes Dirac-Slater wave functions and all necessary multipoles have been computed for C III-VI and Au + 8, +16, +24, and +36 for $n = 1 - 6$ and 10 , $0 \leq l < n$. By use of detailed balance, radiative recombination rate coefficients are obtained for seven temperatures in the range 10 eV - 3 keV from the photoionization cross sections. The cross sections are compared with those obtained by others using semiclassical (Kramers) and hydrogenic models. In most cases, the recombination rate coefficients (summed over subshells) are larger than those computed using hydrogenic photoionization cross sections, by as much as a factor 30 (Au + 8, $n = 5$, $kT = 3$ keV). Analytical fits are given for the rate coefficients summed over l and n . The results are applicable to ionization balance and ion transport calculations for fusion reactors and the solar corona.

I. INTRODUCTION

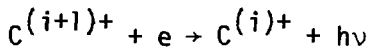
Ionization balance calculations for high-temperature plasmas that occur in the solar corona and in some controlled thermonuclear reactors (CTR), such as Tokamaks, require radiative recombination cross sections or rate coefficients for highly stripped ions. Results are reported here for ions of carbon, important in the solar corona and also expected to be a significant impurity in CTR plasmas, and for gold, a probable impurity in CTR plasmas. Results for Fe XV - XXV ions are reported elsewhere.¹

II. METHOD

Detailed balance arguments² give a relation

$$\sigma_c^{nl}(v) = \frac{g_i}{g_i + 1} \frac{h^2 v^2}{p^2 c^2} \sigma_i^{nl}(v) \quad (1)$$

between the partial cross section $\sigma_c^{nl}(v)$ for the radiative recombination process



and the partial cross section $\sigma_i^{nl}(v)$ for the inverse process, i.e., photoionization from the subshell with binding energy $\epsilon_{nl,i}$. g_i = statistical weight (degeneracy) of configuration $C^{(i)+}$. p = free electron momentum. The other symbols have their usual meanings. The corresponding recombination rate coefficient (cm^3/s) is given by the thermal average

$$\alpha_i^{nl}(kT) = \left\langle \sigma_i^{nl} v \right\rangle ,$$

which, in view of Eq. (1), can be written as an integral over the photoionization cross section.³

$$\alpha_i^{nl}(kT) = \frac{g_i}{g_i + 1} \sqrt{\frac{2}{\pi}} c^{-2} (mkT)^{-3/2} \exp(-\epsilon_{nl,i}/kT) \int_{\epsilon_{nl,i}}^{\infty} (hv)^2 \sigma_i^{nl}(v) e^{-\frac{hv}{kT}} d(hv). \quad (2)$$

When induced recombination is important, a factor $1 + (c^3 U_v / 8\pi h\nu^3)$ should be included in the integral in Eq. (1).⁴ ($U_v dv$ = energy density of the photon field.) The rate coefficients calculated here do not include this factor. The statistical weight of a configuration with partially filled shells is given by⁵

$$g = \prod_{\text{open sub-shells}} \binom{4\ell + 2}{N_\ell} ,$$

where N_ℓ is the number of electrons in subshell ℓ . The ratio of statistical weights that occurs in Eq. (1) is

$$g_i/g_{i+1} = \binom{4\ell + 2}{N_\ell} / \binom{4\ell + 2}{N_\ell - 1} = \frac{4\ell + 3 - N_\ell}{N_\ell} ,$$

N_ℓ being the occupation after recombination.

The computer program PELEC developed by Brysk and Zerby⁶ was used to calculate partial photoionization cross sections for positive ions of carbon and gold. In the single-electron model, the bound-free matrix element is

$$M = - e \int \vec{A}_q \cdot \vec{\psi}_f^+(E) \vec{\alpha} \vec{\psi}_i(E') dV , \quad (3)$$

where $\vec{\alpha}$ is the Dirac matrix operator and the subscripts i and f refer to initial (bound) and final (free) states of the electron. The photon wave is represented by a multipole expansion,

$$\hat{A}_q = - \hat{p} \hat{\xi}_p \frac{4\pi}{2\hbar\nu} e^{iqz} = - \hat{p} \hat{\xi}_p \frac{4\pi}{2\hbar\nu} \sum_{\ell} i^{\ell} [4\pi(2\ell + 1)]^{1/2} Y_{\ell,0}(\hat{r}) j_{\ell}(qr) . \quad (4)$$

Here $\hbar\nu$, q = photon energy and momentum, Y = spherical harmonic, j = spherical Bessel function, $\hat{\xi}_p$ = spherical basis vector, and $p = \pm 1$ corresponding to {right}-left circular polarization. Enough multipoles were used to ensure a calculated cross section converged to within $\pm 1\%$. Dirac-Slater SCF wave functions were obtained using the HEX computer program developed by Liberman et al.⁷

Binding energies for carbon ions were taken from Lotz's compilation;⁸ for gold ions, values computed using HEX were used.*

To facilitate evaluation of the integral in Eq. (2), it was assumed that the resulting cross-section curves can be well approximated by piecewise continuous power-law segments, straight line segments on a log-log plot.

$$\sigma^{nl}(hv) \approx \sigma_k^{nl} (v/v_k)^{B_k^{nl}} \quad (v_{k-1} \leq v \leq v_k, k = 1, 2, \dots) .$$

The integral is then evaluated in terms of incomplete gamma functions.

$$\int_{hv_{k-1}}^{hv_k} (hv)^2 \sigma(v) e^{-hv/kT} d hv \approx \sigma_k u_k^{-B_k} (kT)^3 \left[\Gamma(B_k + 3, u_{k-1}) - \Gamma(B_k + 3, u_k) \right] \quad u_k \equiv hv_k/kT .$$

(The nl has been omitted in the last equation.)

The PELEC program was tested by comparing bound-free Gaunt factors calculated for hydrogenic C VI with results published by Karzas and Latter,⁹ who evaluated the matrix element, Eq. (3), analytically in the nonrelativistic, nonretardation dipole approximation. For this comparison, the PELEC calculation was

* It was found empirically that the cross section for photoionization from an excited orbital, such as $6p_{1/2}$ in the configuration $5s^2 6p_{1/2}$ or $5s5p_{1/2} 6p_{1/2}$ of Au^{+16} , is given with small error by using the wave function for the corresponding orbital in the ground state configuration ($5s^2 5p_{1/2}$ in the example). Therefore, it was unnecessary to calculate wave functions for all possible excited configurations. For carbon ions, however, wave functions were computed for all excited configurations. For each excited configuration, the bound (initial) state function and free (final) state function were obtained using the (self-consistent) potential corresponding to the initial state. For certain initial configurations of C III ($2s6d_{3/2}$, $2s10d_{3/2}$), tests were made using separate potentials for initial and final states. (The final state potential corresponded to the charge distribution $\rho(r)$ for the 2s configuration of C IV, with the Kohn-Sham factor $\alpha = 2/3$ in the exchange term replaced by $0.65 \times 2/3$, following a suggestion by R. D. Cowan, and the "latter tail correction" set to zero.) The cross sections thus obtained are within 10% of those obtained using the single-potential model.

restricted to the "dipole approximation" by limiting the sum in Eq. (4) to $\ell = 0$ and $\ell = 1$ terms and approximating $j_0 \approx 1$, $j_1 \approx 1/2$ qr. The Gaunt factors, defined as the ratio of the cross section to the classical (Kramers) bound-free cross section, Karzas and Latter's Eq. (39), are shown in Fig. 1. The figure also shows cross sections obtained using the full relativistic matrix element, Eq. (3). In Fig. 2, PELEC results for photoionization from the $2p_{1/2}$ subshells of O III and IV are compared with close-coupling calculations.¹⁰ PELEC results have also been compared with other single-electron model calculations¹¹ and with measurements for neutral atoms.¹²

III. RESULTS

Examples of partial photoionization cross sections calculated on the basis of the (nonhydrogenic) single-electron model are shown in Figs. 3 and 4 for C III and in Fig. 5 for Au + 8.* Figures 6-9 show the ratios of the recombination rate coefficients $\sum_{\ell} \alpha_{n\ell}^{nl}$ (summed over partially filled subshells) to the classical Kramers model value,

$$\sum_{\ell} \alpha_{n\ell}^{nl}(T) = (2.6 \times 10^{-14} \text{ cm}^3/\text{s}) n^{-1} \sum_{\ell} N_{n\ell} (g_i/g_{i+1}) \epsilon_{n\ell}^{1/2} q_{n\ell}^{3/2} \exp(q_{n\ell}) E_1(q_{n\ell}) .$$

($q_{n\ell} = \epsilon_{n\ell}/kT$, $\epsilon_{n\ell} = |\text{binding energy (Ryd)}|$, $E_1(x) = \text{exponential integral function.}$) Figures 10-13, similar to Figs. 6-9, show the ratios of $\sum_{\ell} \alpha_{n\ell}^{nl}(T)$ to hydrogenic values. (For the results shown in Figs. 5-12, the Kramers and hydrogenic rate coefficients were calculated using hydrogenic binding energies, i.e., Z^2/n^2 Ryd, with $Z = \text{ion charge before recombination.}$) The partial photoionization cross sections and recombination rate coefficients for individual subshells are available on punched cards by request from LASL Group T-4. Tables I and II are partial computer listings of the cards for a typical case (C IV).

*For subshells that are empty in the ground state configuration, only the partial cross section corresponding to $j = \ell - 1/2$ was computed. In such cases, the partial cross section corresponding to $j = \ell + 1/2$ differs by < 10%.

Values of the partial photoionization cross sections for large values of the principal quantum number n (and small l) can be extrapolated from the PELEC results at smaller n by Lee and Pratt's method,¹³ which is based on quantum defect theory. Partial cross sections for C VI $n = 10$, $0 \leq l \leq 3$, extrapolated from the PELEC results for $n = 4$ and 6 are given in Table III.*

For principal quantum number n large enough so that the hydrogenic approximation is valid, an expression that Seaton¹⁴ derived for $\sum_{n'=n}^{\infty} \sum_{l=0}^{\infty} \alpha^{n'l}$ is useful.

More crudely, values of α^n/α_{Kr}^n ($\alpha^n = \sum_l \alpha^{nl}$) can be interpolated between the value that corresponds to the largest n for which results are given here, and the value 1.0 assumed to hold for large enough n , say $n > 100$ (Fig. 14). Values of $\sum_{l=0}^{100} \alpha^n(T)$ so calculated are given in Table IV. For C VI, the value of $\sum_{l=6}^{\infty} \alpha^n(T)$ so calculated agrees within 2% with the result obtained for $\sum_{l=6}^{\infty}$ using Seaton's formulas. See Fig. 15.

Coefficients for analytical approximations of the form

$$10^P kT(\text{kev}) \sum \alpha^n(T) = \sum_{j=1}^J b_j \left\{ \log_{10}[kT(\text{kev})] \right\}^{j-1} \quad (5)$$

are displayed in Tables V-VI. In the case of C ions the maximum deviation of the fits is 1%.

Summers¹⁵ calculated ionization equilibria for carbon plasmas. The rate coefficients reported here, summed over empty and partially filled subshells, are compared with Summers' "effective dielectronic-collision rate coefficients" in Figs. 16-18. The comparison indicates that for some conditions radiative recombination is competitive with the dielectronic recombination process.

*These data are given to supplement Karzas and Latter's⁹ hydrogenic model results. Note that the extrapolation method is useful only for values of $h\nu > \max(\epsilon_1, \epsilon_2)$, where ϵ_1 and ϵ_2 are binding energies that correspond to the values of n on which the extrapolation is based.

The results reported here represent use of an improved, nonhydrogenic model and are a contribution to the atomic data base required for ionization balance calculations that are more refined than those reported by others,¹⁶⁻¹⁸ who used hydrogenic or classical model rate coefficients.*

ACKNOWLEDGMENT

The least-squares fits were made by David P. Martinez.

REFERENCES

1. W. D. Barfield, Nucl. Fusion 15, 1192 (1975).
2. J. W. Bond, K. M. Watson, and J. A. Welch, Jr., Atomic Theory of Gas Dynamics (Addison-Wesley Publishing Co., 1965).
3. D. R. Bates and A. Dalgarno, in Atomic and Molecular Processes, D. R. Bates, Ed. (Academic Press, 1962).
4. Ya.B. Zel'Dovich and Yu.P. Raizer, Physics of Shock Waves and High-Temperature Hydrodynamic Phenomena (Academic Press, 1966).
5. R. D. Cowan, J.O.S.A. 58, 815 (1968).
6. H. Brysk and C. D. Zerby, Phys. Rev. 171, 292 (1968).
7. D. A. Liberman, D. T. Cromer, and J. T. Waber, Comput. Phys. Commun. 2, 107 (1971).
8. W. Lotz, Inst. für Plasmaphysik report IPP 1/56 (1967).
9. W. J. Karzas and R. Latter, Astrophys. J. Suppl. 55, 167 (1961).
10. R. J. W. Henry, Astrophys. J. 161, 1153 (1970).
11. E. J. McGuire, Phys. Rev. 175, 20 (1968).
12. W. D. Barfield, G. D. Koontz, and W. F. Huebner, J. Quant. Spectrosc. Radiat. Transfer 12, 1409 (1972).
13. C. M. Lee and R. H. Pratt, U. of Pittsburgh, Physics Dept. report PITT-149 (1975).
14. M. J. Seaton, Mon. Not. Roy. Astr. Soc. 119, 81 (1959).

*Tarter¹⁹ published recombination rate coefficients for temperatures $\gtrsim .05$ keV for a number of light ions calculated using nonhydrogenic photoionization cross sections for valence shells and hydrogenic values for higher shells.

15. H. P. Summers, Appleton (Culham) Laboratory report AL-IM-367 (1974).
16. C. Jordan, Mon. Not. Roy. Astron. Soc. 142, 501 (1969).
17. A. Burgess and H. P. Summers, Astrophys. J. 157, 1007 (1969).
18. I. L. Beigman et al., Astron. Zh. 46, 985 (1969).
19. C. B. Tarter, Astrophys. J. 168, 313 (1971).

TABLE I
CARDS CONTAINING PHOTOIONIZATION CROSS-SECTION DATA FOR TYPICAL CASE C IV

For each subshell, the first card has four integers that represent subshell sequence number, orbital angular momentum quantum number ℓ , occupation number, and principal quantum number n . In some cases, the binding energy (in keV) from LOTZ's tables⁸ is given in floating-point print format. Succeeding cards show the values of $h\nu$ (keV) and $\sigma_{n\ell j}$ (Barns). (Two sets of values with the same n , ℓ correspond to $j = \ell - 1/2$ and $j = \ell + 1/2$.) All values of $h\nu$ should be increased by B.E. (LOTZ) - $h\nu_0$, where $h\nu_0$ is the lowest value tabulated for a particular subshell.

10	0	2			
1	0	2	1	0,343	
3,2768E+01	6,4822E+05	1	0		C IV
5,0000E+01	2,4496E+05	1	4		C IV
1,0000E+00	3,9085E+04	1	4		C IV
2,0000E+00	5,3684E+03	1	4		C IV
5,0000E+00	3,3419E+02	1	6		C IV
1,0000E+01	3,7351E+01	1	6		C IV
2,0000E+01	3,9394E+00	1	6		C IV
2	0	1	2	0,0645	
6,3756E+02	6,4607E+05	2	0		C IV
1,0000E+01	2,9285E+05	2	3		C IV
2,0000E+01	7,0869E+04	2	3		C IV
5,0000E+01	8,1321E+03	2	4		C IV
1,0000E+00	1,3375E+03	2	4		C IV
2,0000E+00	1,9695E+02	2	4		C IV
5,0000E+00	1,2791E+01	2	6		C IV
1,0000E+01	1,4625E+00	2	6		C IV
2,0000E+01	1,5646E-01	2	6		C IV
3	1	1	2		
5,5543E+02	9,1571E+05	3	0		C IV
1,0000E+01	1,5377E+05	3	3		C IV
2,0000E+01	1,6945E+04	3	3		C IV
5,0000E+01	8,0590E+02	3	4		C IV
1,0000E+00	7,3086E+01	3	4		C IV
2,0000E+00	5,6209E+00	3	4		C IV
5,0000E+00	1,3877E-01	3	6		C IV
1,0000E+01	8,6742E-03	3	6		C IV
2,0000E+01	4,8499E-04	3	6		C IV

TABLE I (cont)

5	0	1	3		
2.6778E-02	1.0400E+06	5	0	C	IV
5.0000E-02	3.4165E+05	5	3	C	IV
1.0000E-01	8.6881E+04	5	3	C	IV
2.0000E-01	1.9401E+04	5	3	C	IV
5.0000E-01	2.1684E+03	5	4	C	IV
1.0000E+00	3.5761E+02	5	4	C	IV
2.0000E+00	5.3010E+01	5	4	C	IV
5.0000E+00	3.4596E+00	5	6	C	IV
1.0000E+01	3.9711E-01	5	6	C	IV
2.0000E+01	4.2788E-02	5	6	C	IV
6	1	1	3		
2.4564E-02	1.7272E+06	6	0	C	IV
5.0000E-02	2.8903E+05	6	3	C	IV
1.0000E-01	4.1724E+04	6	3	C	IV
2.0000E-01	5.1120E+03	6	3	C	IV
5.0000E-01	2.6218E+02	6	4	C	IV
1.0000E+00	2.4376E+01	6	4	C	IV
2.0000E+00	1.9814E+00	6	4	C	IV
5.0000E+00	4.7923E-02	6	8	C	IV
1.0000E+01	2.9545E-03	6	8	C	IV
2.0000E+01	1.6679E-04	6	8	C	IV
8	2	1	3		
2.4194E-02	1.1377E+06	8	0	C	IV

TABLE I (cont)

5.0000E+02	8.4004E+04	8	4	
1.0000E+01	5.6268E+03	8	4	C IV
2.0000E+01	3.1145E+02	8	4	C IV
5.0000E+01	5.5342E+00	8	7	C IV
1.0000E+00	2.5265E-01	8	7	C IV
2.0000E+00	1.1628E-02	8	7	C IV
				C IV
10 0	1 4			
1.4669E+02	1.4886E+06	10	0	
2.0000E+02	8.5443E+05	10	3	C IV
5.0000E+02	1.4910E+05	10	3	C IV
1.0000E+01	3.6072E+04	10	3	C IV
2.0000E+01	7.8827E+03	10	3	C IV
5.0000E+01	8.7373E+02	10	4	C IV
1.0000E+00	1.4426E+02	10	4	C IV
2.0000E+00	2.1425E+01	10	4	C IV
5.0 -00	0.1401 -01	10	7	C IV
1.0 +01	0.1611 -00	10	7	C IV
				C IV
11 1	1 4			
1.3770E+02	2.5889E+06	11	0	
2.0000E+02	1.1171E+06	11	3	C IV
5.0000E+02	1.1624E+05	11	3	C IV
1.0000E+01	1.7206E+04	11	3	C IV
2.0000E+01	2.1618E+03	11	3	C IV
5.0000E+01	1.1328E+02	11	4	C IV
1.0000E+00	1.0624E+01	11	4	C IV
2.0000E+00	8.3164E-01	11	4	C IV
5.0 -00	0.2202 -01	11	7	C IV
1.0 +01	0.1306 -02	11	6	C IV
				C IV
13 2	1 4			
1.3609E+02	2.2501E+06	13	0	
2.0000E+02	7.3883E+05	13	4	C IV
5.0000E+02	3.6914E+04	13	4	C IV
1.0000E+01	2.8015E+03	13	4	C IV
2.0000E+01	1.6813E+02	13	4	C IV
5.0000E+01	3.1824E+00	13	12	C IV
1.0 -00	0.1485 -00	13	5	C IV
2.0 -00	0.6910 -02	13	5	C IV
				C IV
15 3	1 4			
1.3606E+02	1.1916E+06	15	0	
2.0000E+02	2.6594E+05	15	4	C IV
5.0000E+02	5.2767E+03	15	4	C IV
1.0000E+01	1.9736E+02	15	4	C IV
2.0000E+01	5.7338E+00	15	4	C IV
5.0000E+01	3.9909E-02	15	12	C IV
				C IV

SFM,
SEJ,

TABLE II
CARDS CONTAINING RECOMBINATION COEFFICIENT DATA
FOR TYPICAL CASE C III -- RECOMBINATION TO C IV

For each subshell are given subshell designation, recombination rate coefficient $\alpha^{n,l}$ (cm³/s), ratio to Kramers value (α/α_{Kr}), ratio of hydrogenic value to Kramers value (α_H/α_{Kr}). (For $4 < n$, the hydrogenic coefficients are averaged over subshells.) "G.T.," and "L.T.," indicate lower and upper bounds, respectively. The data following "sums over subshells," include principal quantum number n ; $\sum_l \alpha^{nl}$ (lower and upper bounds); $\sum_l \alpha^{nl}/\sum_l \alpha^{nl}$ (lower and upper bounds); $\sum_l \alpha_H^{nl}/\sum_l \alpha_{Kr}^{nl}$; and $\sum_l \alpha_{Kr}^{nl}$. Only partially filled subshells are included in the sums. Unless otherwise indicated by a comment card, the Kramers and hydrogenic rate coefficients are calculated using the same binding energies used for the nonhydrogenic model calculation. The upper bounds are estimates based on assumed power-law extrapolation of the photoionization cross section for $h\nu \rightarrow \infty$.

C3 99 KT = 1.0000E-02 KEV			1.2242E-01		
		ALFA (CM ³ /S)	ALFA/ALFA(KR)	ALFA(H)/ALFA(KR)	
1	1S	8.9123E-13	3.5142E+00	8.0305E-01	9.9220F-01
2	2S	4.0939E-14	1.5205E+00	1.1246E+00	9.9220E-01
3	2P	2.3700E-13	1.4671E+00	8.2315E-01	9.9220F-01
4	3S	1.9371E-14	1.4638E+00	1.5061E+00	9.9220F-01
5	3P	7.9944E-14	2.0137E+00	1.2548E+00	9.9220F-01
6	3D	5.0486E-14	7.6302E-01	6.1524E-01	9.9220F-01
7	4S	8.0609E-15	1.7362E+00	9.6081E-01	9.9220F-01
8	4P	3.3472E-14	2.4003E+00	9.6241E-01	9.9220F-01
9	4D	3.7379E-14	1.6102E+00	9.6780E-01	9.9220F-01
10	4F	1.3138E-14	4.0425E-01	9.6288E-01	9.9220F-01
11	6S	2.4874E-15	2.5235E+00	9.8569E-01	9.9220F-01
12	6P	1.0485E-14	3.5527E+00	9.8569E-01	9.9220E-01
13	6O	1.4806E-14	3.0101E+00	9.8558E-01	9.9220E-01
14	6F	9.6682E-15	1.4040E+00	9.8558E-01	9.9220E-01
15	6G	4.4503E-15	5.0246E-01	9.8558E-01	9.9220E-01
16	6H	1.2469E-15	1.1523E-01	9.8558E-01	9.9220E-01
17	10S	5.3806E-16	4.3457E+00	9.9491E-01	9.9220E-01
18	10P	2.3516E-15	6.3203E+00	9.9498E-01	9.9220E-01
19	10D	3.4049E-15	5.4940E+00	9.9493E-01	9.9220E-01
20	10F	3.2813E-15	3.7796E+00	9.9497E-01	9.9220F-01
21	10G	2.1547E-15	1.9304E+00	9.9499E-01	9.9220E-01
22	10H	1.3722E-15	1.0058E+00	9.9500E-01	9.9220E-01
23	10I	7.6152E-16	4.7232E-01	9.9583E-01	9.9220F-01
24	10K	3.5353E-16	1.9004E-01	9.9488E-01	9.9220E-01
25	10L	1.1502E-16	5.4552E-02	9.9481E-01	9.9220F-01
26	10M	2.0114E-17	8.5360E-03	9.9499E-01	9.9220E-01

TABLE II (cont)

SUMS OVER SUBSHELLS

N	SUM ALFA (CM3/S)	(SUM ALFA) /(SUM ALFA(KR))	(SUM ALFA(H)) /(SUM ALFA(KR))	SUM ALFA(KR)
2	2.77937E-13	2.77937E-13	1.47471E+00	1.47471E+00
3	1.49801E-13	1.49801E-13	1.25777E+00	1.25777E+00
4	9.20099E-14	9.20099E-14	1.23863E+00	1.23863E+00
6	4.31380E-14	4.31380E-14	1.21809E+00	1.21809E+00
10	1.43559E-14	1.43560E-14	1.15752E+00	1.15753E+00

H-GENIC B.E.S WITH Z = 3 USED FOR KRAMERS AND H-GENIC C.S. AND RATE COEFFS.

C3 99 KT = 3.0000E-02 KEV

4.0000E-02

		ALFA (CM3/S)	ALFA/ALFA(KR)	ALFA(H)/ALFA(KR)
1	1S	4.9817E-13	3.8199E+00	8.2121E-01
2	2S	2.4744E-14	2.0928E+00	1.3480E+00
3	2P	1.1140E-13	1.5732E+00	7.8240E-01
4	3S	1.2349E-14	2.3892E+00	2.0013E+00
5	3P	3.8999E-14	2.5151E+00	1.3315E+00
6	3D	1.7295E-14	6.6885E-01	5.1041E-01
7	4S	5.0253E-15	3.0135E+00	9.8472E-01
8	4P	1.6114E-14	3.2210E+00	9.8583E-01
9	4D	1.3245E-14	1.5709E+00	9.8417E-01
10	4F	3.5849E-15	3.0710E+01	9.8425E+01
11	5S	1.5130E-15	4.7750E+00	1.0049E+00
12	5P	5.0552E-15	5.3182E+00	1.0050E+00
13	6D	5.2994E-15	3.3451E+00	1.0049E+00
14	6F	2.7058E-15	1.2200E+00	1.0049E+00
15	6G	1.0601E-15	3.7175E+01	1.0049E+00
16	6H	2.7388E-16	7.8580E-02	1.0049E+00
17	10S	3.1601E-16	8.8852E+00	1.0107E+00
18	10P	1.1005E-15	1.0294E+01	1.0107E+00
19	10D	1.2017E-15	6.7496E+00	1.0107E+00
20	10F	9.3310E-16	3.7773E+00	1.0109E+00
21	10G	5.1634E-16	1.6095E+00	1.0108E+00
22	10H	3.0136E-16	7.6812E-01	1.0108E+00
23	10I	1.5994E-16	3.4494E-01	1.0114E+00
24	10K	7.2034E-17	1.3454E-01	1.0106E+00
25	10L	2.3041E-17	3.8001E-02	1.0105E+00
26	10M	3.9836E-18	5.8783E-03	1.0108E+00

SUMS OVER SUBSHELLS

N	SUM ALFA (CM3/S)	(SUM ALFA) /(SUM ALFA(KR))	(SUM ALFA(H)) /(SUM ALFA(KR))	SUM ALFA(KR)
2	1.36344E-13	1.36344E-13	1.64742E+00	1.64742E+00
3	6.86331E-14	6.86331E-14	1.47543E+00	1.47543E+00
4	3.79893E-14	3.79893E-14	1.42380E+00	1.42380E+00
6	1.59074E-14	1.59074E-14	1.39459E+00	1.39459E+00
10	4.63087E-15	4.63508E-15	1.29835E+00	1.29953E+00

H-GENIC B.E.S WITH Z = 3 USED FOR KRAMERS AND H-GENIC C.S. AND RATE COEFFS.

TABLE III
 PARTIAL PHOTOIONIZATION CROSS SECTIONS FOR C VI ($n = 10$, $0 \leq l \leq 3$)
 EXTRAPOLATED FROM $n = 4$ AND 6 BY LEE AND PRATT'S METHOD¹³

Partial Cross Section (Barns) ($n = 10$)

<u>$h\nu$ (keV)</u>	<u>$l = 0$</u>	<u>$l = 1$</u>	<u>$l = 2$</u>	<u>$l = 3$</u>
0.031 ^a	7.24 + 4	6.43 + 4	4.57 + 4	2.64 + 4
0.05	2.57	2.13	1.32	6.09 + 3
0.1	5.50 + 3	3.61 + 3	1.54 + 3	4.28 + 2
0.2	1.12	5.24 + 2	1.37 + 2	2.06 + 1
0.5	1.20 + 2	2.99 + 1	3.47 - 0	2.22 - 1
1.0	1.94 + 1	2.73 - 0	1.66 - 1	5.42 - 3
2.0	2.78 - 0	2.13 - 1	7.68 - 3	
5.0	1.80 - 1	6.56 - 3		
10.0	2.07 - 2	3.93 - 4		
20.0	2.30 - 3	1.83 - 5		
50.0	1.25 - 4			
100.0	1.30 - 5			
200.0	1.70 - 6			

^aB.E. = 4.9 eV.

TABLE IV
 SUMS OVER PARTIALLY FILLED SHELLS ($n < 99$) of RADIATIVE
 RECOMBINATION COEFFICIENTS (cm^3/s) FOR GOLD AND CARBON IONS

<u>kT (keV)</u>	<u>AU⁺⁸</u>	<u>AU⁺¹⁶</u>	<u>AU⁺²⁴</u>	<u>AU⁺³⁶^a</u>
0.1	6.69 - 13	5.20 - 12	1.90 - 11	5.27 - 11
0.3	5.50 - 13	2.90 - 12	9.05 - 12	2.40 - 11
1.0	4.13 - 13	1.55 - 12	3.88 - 12	9.51 - 12
3.0	2.18 - 13	7.70 - 13	1.65 - 12	3.74 - 12
	<u>C III</u>	<u>C IV</u>	<u>C V</u>	<u>C VI^b</u>
0.01	8.05 - 13	1.40 - 12	3.17 - 12	5.40 - 12
0.03	3.40 - 13	5.79 - 13	1.43 - 12	2.52 - 12
0.1	1.19 - 13	2.03 - 13	5.66 - 13	1.03 - 12
0.3	4.17 - 14	7.12 - 14	2.24 - 13	4.23 - 13
1.0	1.15 - 14	2.04 - 14	7.18 - 14	1.41 - 13
3.0	3.15 - 15	5.84 - 15	2.25 - 14	4.49 - 14

^aI.e., $\text{Au}^{+37} + \text{e} \rightarrow \text{Au}^{+36}$.

^bI.e., $\text{C}^{+6} + \text{e} \rightarrow \text{C}^{+5}$.

TABLE V
 COEFFICIENTS FOR FITS [EQ. (5) OF TEXT] GIVING
 TEMPERATURE DEPENDENCE OF RECOMBINATION RATE COEFFICIENTS
 (SUMMED OVER EMPTY AND PARTIALLY FILLED SHELLS) FOR (cm³/s) IONS. p = 15.

	b ₁	b ₂	b ₃	b ₄
C III	11.61	-3.040	-3.091	-.3379
C IV	20.49	-3.884	-4.754	-.5863
C V	72.06	+0.7815	-19.52	-4.906
C VI	140.8	9.171	-39.05	-10.99

TABLE VI
 COEFFICIENTS FOR FITS [EQ. (5) OF TEXT] GIVING
 TEMPERATURE DEPENDENCE OF RECOMBINATION RATE COEFFICIENTS
 (SUMMED OVER EMPTY AND PARTIALLY FILLED SHELLS) (cm³/s) FOR Au IONS. p = 14.

	b ₁	b ₂	b ₃	max. dev. (%)
Au + 8	39.51	48.43	14.98	11.
Au + 16	152.9	144.6	42.97	2.4
Au + 24	384.2	222.3	26.72	1.4
Au + 36	941.9	395.1	-23.05	1.2

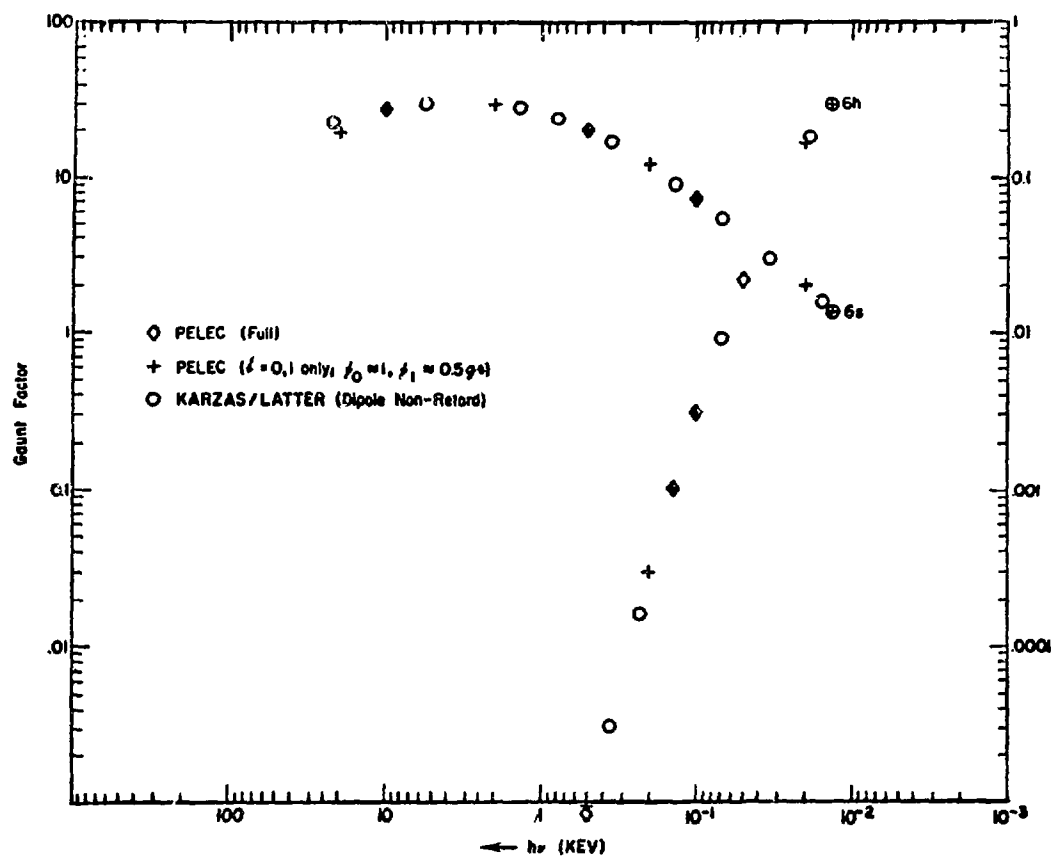


Fig. 1.
 PELEC code results for bound-free Gaunt factor for a hydrogenic ion (C VI, 6S and 6h) are compared with Karzas and Latter's⁹ nonretardation dipole approximation results.

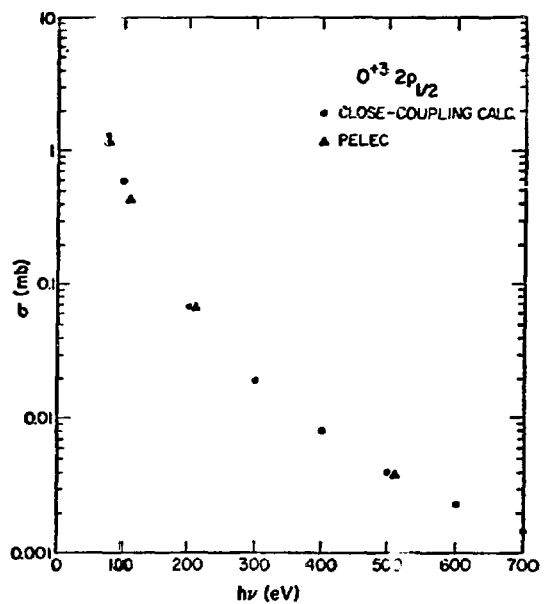
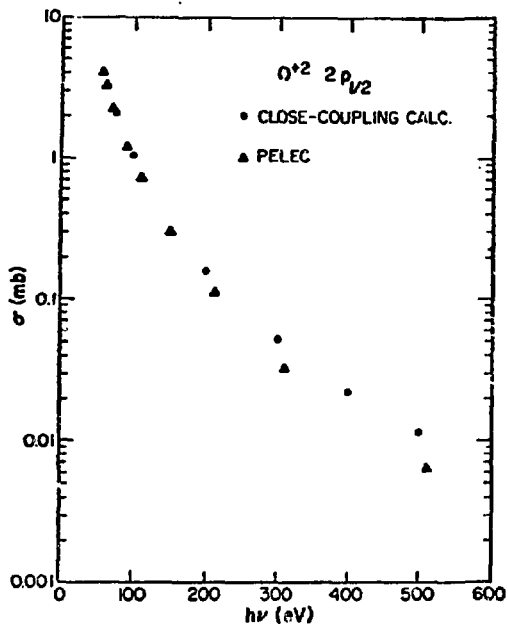


Fig. 2.
Partial cross sections for photoionization of O III and O IV as given by single-electron (PELEC code) and close-coupling¹⁰ models. For O III, the close-coupling model results for 3P , 1D , and 1S configurations have been averaged using the corresponding statistical weights.

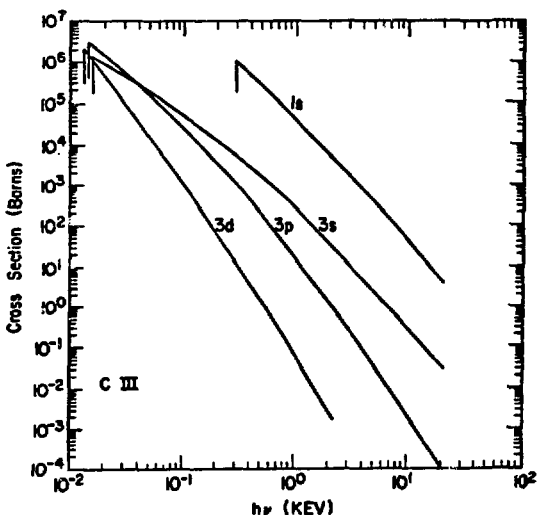


Fig. 3.
Theoretical partial photoionization cross sections for $n = 1$ and $n = 3$ shells of C III, calculated using PELEC.

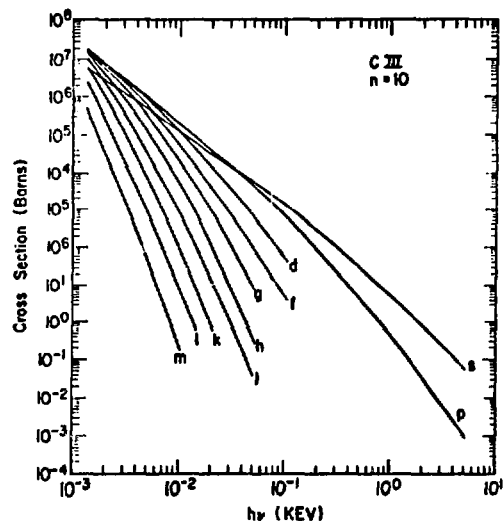


Fig. 4.
Theoretical partial photoionization cross sections for $n = 10$ shell of C III, calculated using PELEC.

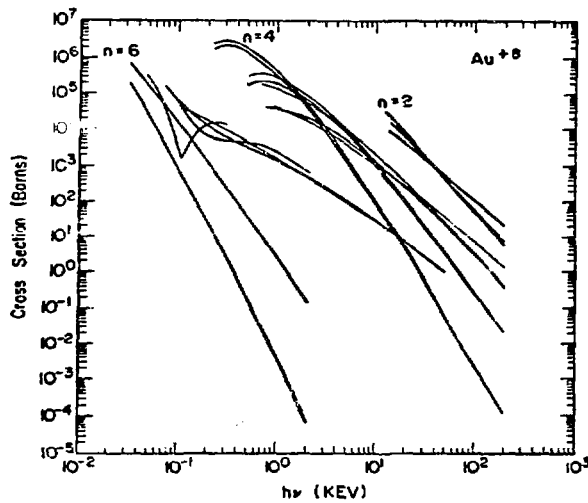


Fig. 5.
Theoretical partial photoionization cross sections for $n = 2, 4$, and 6 shells of Au^{+8} , calculated using PELEC.

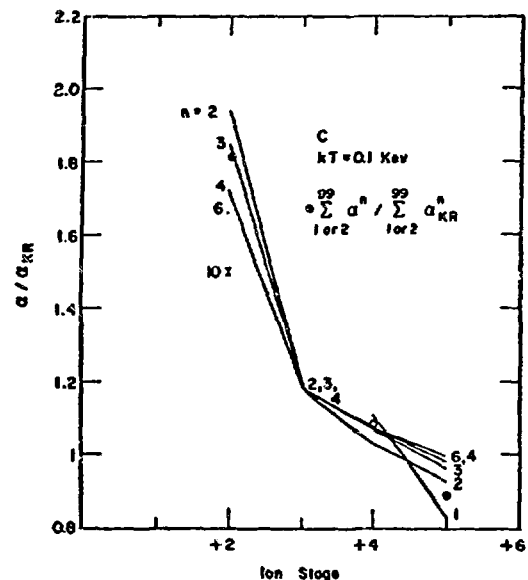


Fig. 6.
Ratio of nonhydrogenic recombination coefficients summed over partially filled subshells to semiclassical Kramers value for C ions ($kT = 0.1$ keV). The Kramers values are based on hydrogenic binding energies. "Ion stage" refers to charge state after recombination.

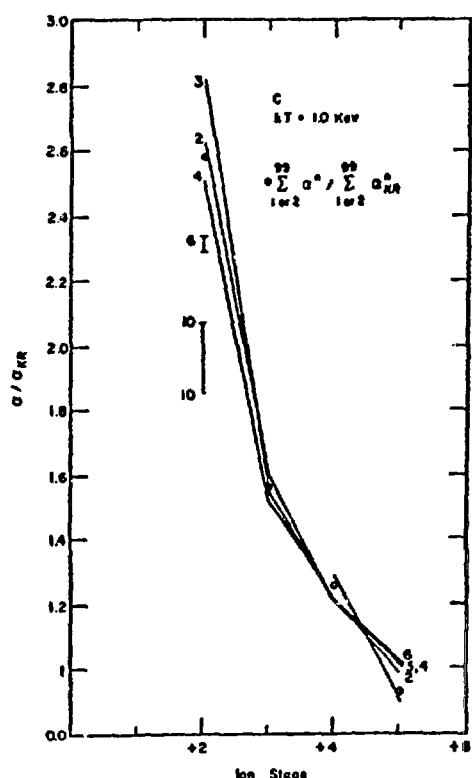


Fig. 7.
Ratio of nonhydrogenic recombination coefficients summed over partially filled subshells to semiclassical Kramers value for C ions ($kT = 1$ keV).

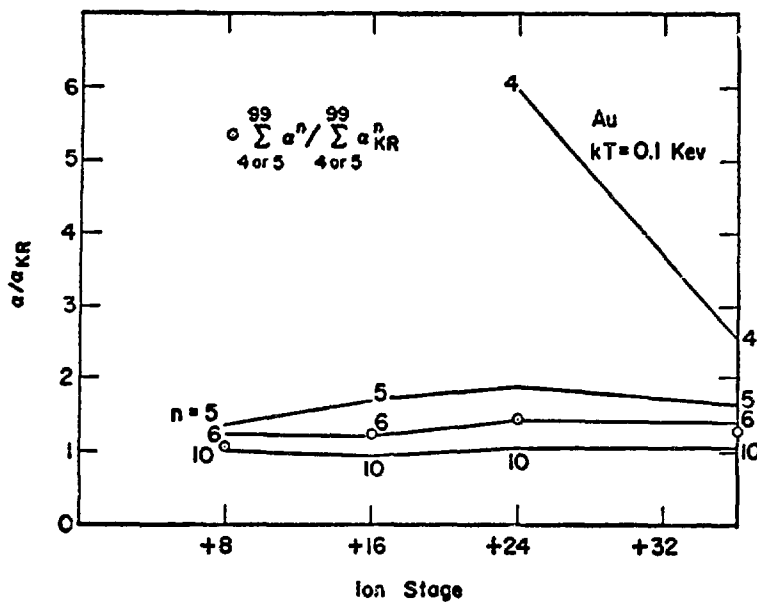


Fig. 8.

Ratio of nonhydrogenic recombination coefficients (summed over partially filled subshells to semiclassical Kramers value for Au ions ($kT = 0.1$ keV).

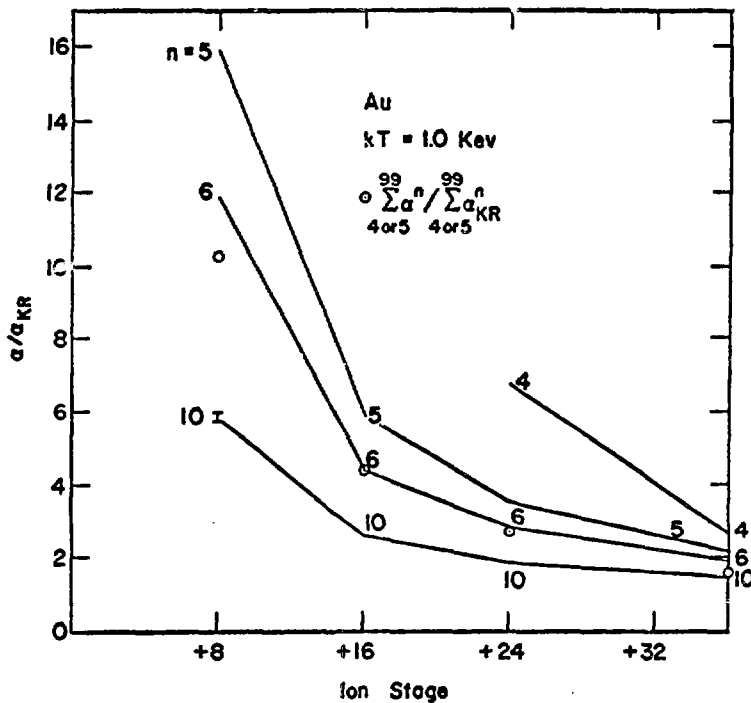


Fig. 9.

Ratio of nonhydrogenic recombination coefficients summed over partially filled subshells to semiclassical Kramers value for Au ions ($kT = 1$ keV).

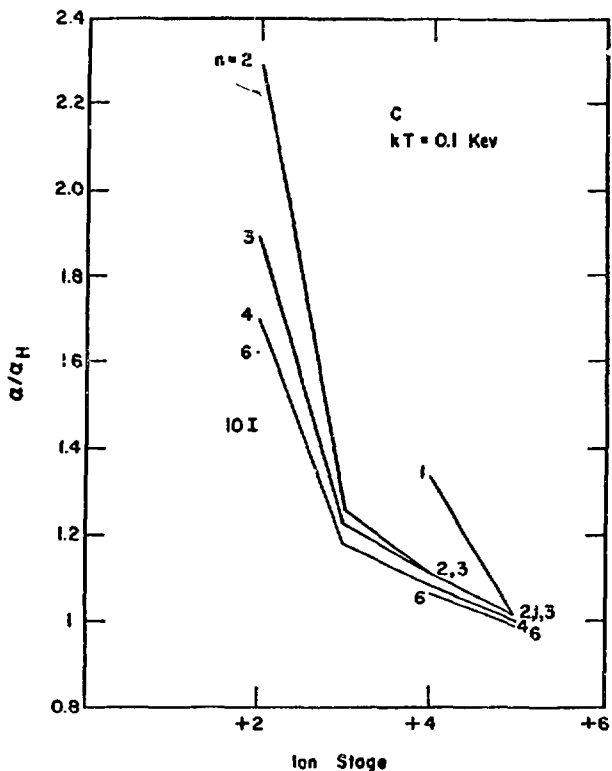


Fig. 10.
Ratio of nonhydrogenic recombination
coefficients summed over partially
filled subshells to hydrogenic value
for C ions ($kT = 0.1$ keV).

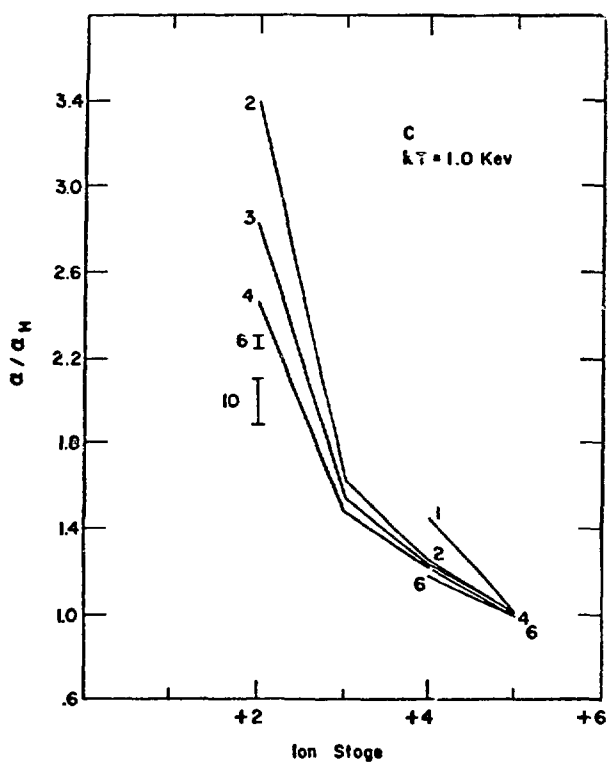


Fig. 11.
Ratio of nonhydrogenic recombination
coefficients summed over partially
filled subshells to hydrogenic value
for C ions ($kT = 1$ keV).

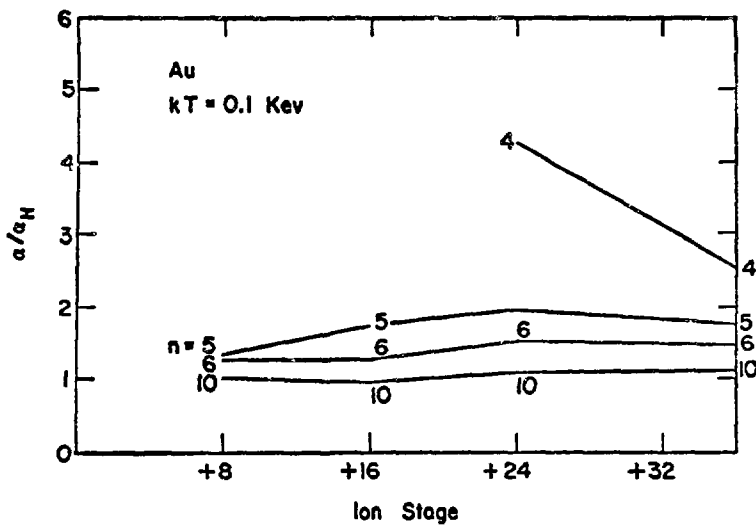


Fig. 12.

Ratio of nonhydrogenic recombination coefficients summed over partially filled subshells to hydrogenic value for Au ions ($kT = 0.1$ keV).

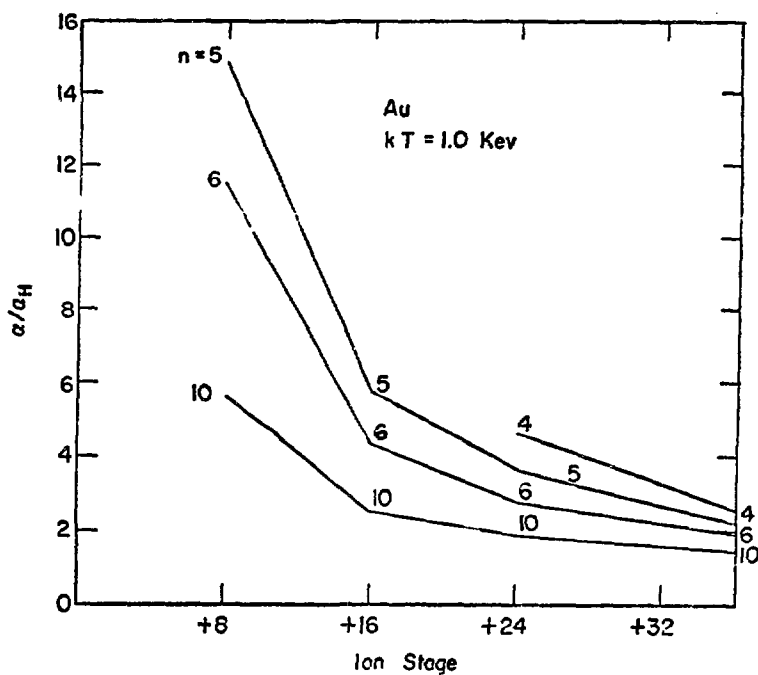


Fig. 13.

Ratio of nonhydrogenic recombination coefficients summed over partially filled subshells to hydrogenic value for Au ions ($kT = 1$ keV).

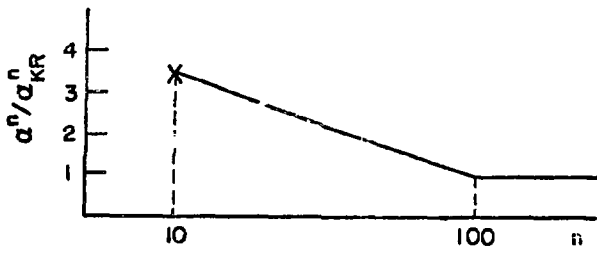


Fig. 14.
Illustrates method for extrapolating recombination coefficients to large values of n .

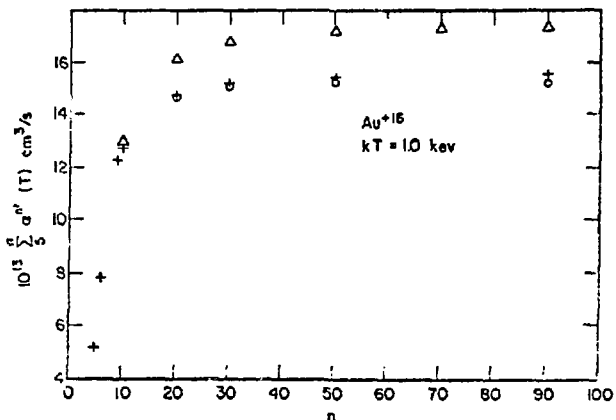


Fig. 15.
Sum of recombination coefficients for Au\$^{+16}\$ ($kT = 1.0$ keV). $\alpha_{N_2}^n/\alpha_{Kr}^n = 1.0$, by hypothesis. ($\alpha^n = \sum_l \alpha^{nl} (T)$). Values of α^n/α_{Kr}^n for $N_0 < n < N_1$, and $N_1 < n < N_2$ are obtained by interpolation. (0) $N_0 = 5, N_1 = 10, N_2 = 50$; (+) $N_0 = 5, N_1 = 10, N_2 = 100$; (\$\Delta\$) $N_0 = 5, N_1 = 6, N_2 = 100$.

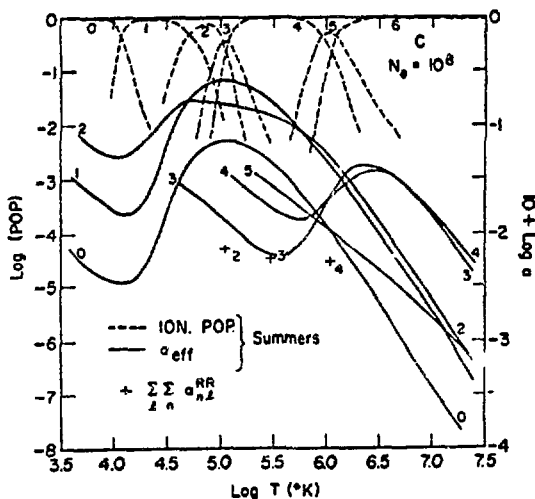


Fig. 16.
Radiative recombination rate coefficients summed over partially filled subshells with $n = 1$ to 99 are compared with Summers' "effective dielectronic-collision rate coefficients" for carbon plasma with $N_e = 10^8/\text{cm}^3$. Also shown are Summers' calculated ion populations (dashed curves).

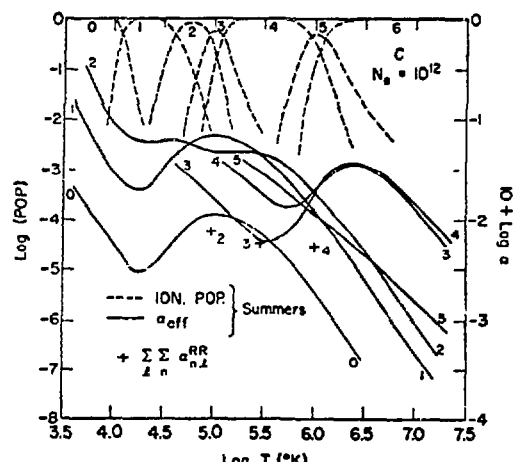


Fig. 17.
Radiative recombination rate coefficients summed over partially filled subshells with $n = 1$ to 99 are compared with Summers' "effective dielectronic-collision rate coefficients" for carbon plasma with $N_e = 10^{12}/\text{cm}^3$. Also shown are Summers' calculated ion populations (dashed curves).

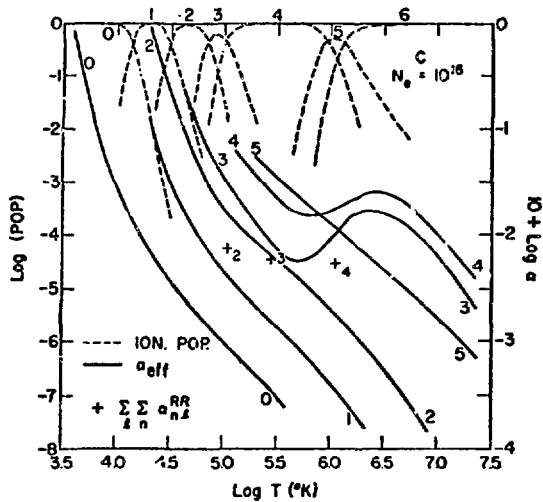


Fig. 18.

Radiative recombination rate coefficients summed over partially filled subshells with $n = 1$ to 99 are compared with Summers' "effective dielectronic-collision rate coefficients" for carbon plasma with $N_e = 10^{16}/\text{cm}^3$. Also shown are Summers' calculated ion populations (dashed curves).